DOI: 10.15669/pnst.5.112

Progress in Nuclear Science and Technology
Volume 5 (2018) pp. 112-115

ARTICLE

Single crystal growth and fermi surface properties in $ThSb_2$ and $ThBi_2$

Ai Nakamura[a*], Fuminori Honda[a], Yoshiya Homma[a], Dexin Li[a], Dai Aoki[a], Hisatomo Harima[b] and Yoshichika Ōnuki[c]

[a]*Institute for Materials Research, Tohoku University, Oarai, Ibaraki, 311-1313, Japan;* [b]*Graduate School of Science, Kobe University, Kobe, 657-8501, Japan;* [c]*Faculty of Science, University of the Ryukyus, Nishihara, Okinawa, 903-0213, Japan*

We grew high-quality single crystals of $ThSb_2$ and $ThBi_2$ and carried out the de Haas-van Alphen (dHvA) measurement and the full-potential LAPW band calculation. Detected main dHvA branches named α and α′ correspond to an electron Fermi surface, while branch β corresponds to a main hole Fermi surface. Each Fermi surface shows approximately the same cross-sectional areas for $ThSb_2$ and $ThBi_2$. On the other hand, the corresponding cyclotron effective masses of $ThBi_2$ are larger than those of $ThSb_2$, which is approximately consistent with a ratio of an electronic specific heat coefficient γ of $ThBi_2$ to that of $ThSb_2$, $\gamma_{ThBi2}/\gamma_{ThSb2} = 1.4$. This might be due to a small band width of $ThBi_2$, compared with the one of $ThSb_2$, reflecting large lattice constants of $ThBi_2$, compared with those of $ThSb_2$.

Keywords: $ThSb_2$; $ThBi_2$; dHvA; Fermi surface; energy band calculation

1. Introduction

The 5*f*-electrons in a magnetic uranium compound possess dual nature: localized and itinerant features. Namely, the 5*f* electrons contribute to the volume of the Fermi surface and also to a magnetic moment at the uranium sites [1]. A non-5*f* thorium compound does not become a reference compound for the corresponding uranium compound because valence electrons of the Th atom, $6d^27s^2$, are different from $5f^36d^17s^2$ or $5f^26d^27s^2$ of the U atom. The number of valence electrons in the thorium compound is, however, the same as that of a 4*f*-itinerant cerium compound. The topology of the Fermi surface in $ThRhIn_5$ [2] is approximately the same as in 4*f*-itinerant $CeCoIn_5$ [3], for example. The cyclotron effective masses are, however, significantly different between $ThRhIn_5$ and $CeCoIn_5$. Large cyclotron masses in $CeCoIn_5$ are due to the many-body Kondo effect.

In the present study, we grew single crystals of $ThSb_2$ and $ThBi_2$ with the tetragonal structure by the self-flux method and studied the Fermi surface properties. The experimental purpose of the present study is to clarify the electronic properties of Sb-5*p* and Bi-6*p* electrons and also a small contribution of Th-5*f* electrons to conduction electrons.

2. Experimental procedure

Single crystals of $ThSb_2$ and $ThBi_2$ with the anti-Cu_2Sb-type tetragonal structure (No. 129, D^7_{4h}, *P*4/*nmm*), were grown by Sb and Bi self-flux method, respectively. Starting materials of 2N(99% pure)-Th, 6N-Sb, and 4N-Bi, with concentration of Th:Sb(Bi)=1:9, were inserted in an alumina crucible. The crucible was encapsulated in a quartz ampoule, heated to 1100 °C, slowly cooled to 300 °C, taking 12 days, and finally cooled to room temperature. The size of an obtained plate-like single crystal was about $1 \times 2 \times 0.3$ mm^3 in $ThSb_2$, revealing a flat tetragonal (001) plane, as shown in **Figure 1(a)**. $ThBi_2$ is also obtained as a thin plate with a much large size, as shown in **Figure 1(b)**. To confirm the sample quality, we measured the electrical resistivity. The residual resistivity ρ_0 is 0.3 μΩ·cm and the residual resistivity ratio RRR (= ρ_{RT}/ρ_0, ρ_{RT}: resistivity at room temperature) is 85 for $ThSb_2$, and ρ_0 = 0.7 μΩ·cm and RRR = 37 for $ThBi_2$, indicating high-quality samples.

The orientation of the single crystal sample of $ThSb_2$ and $ThBi_2$ were determined by the X-ray Laue method. We also determined the lattice parameters and atomic positions of $ThSb_2$ at room temperature. The small

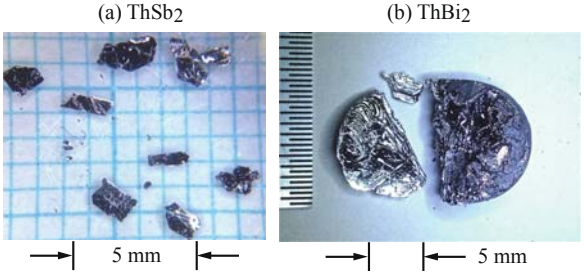

Figure 1. Single crystal ingots of (a) $ThSb_2$ and (b) $ThBi_2$.

*Corresponding author. Email: nakamuraai@imr.tohoku.ac.jp

single crystal sample was mounted on a glass fiber. The measurements were performed on a CCD detector with graphite monochromated Mo-Kα radiation. We summarize in **Table 1** the crystal structure data in $ThSb_2$. These values are in good agreement with the previous data of a = 4.344 Å, c = 9.154 Å, and z = 0.27 for Th (2c) and 0.63 for Sb2 (2c) [4]. We cannot, however, determine the crystal structure data in $ThBi_2$ because of intensive oxidization of the sample. It is reported that a = 4.492 Å, c = 9.298 Å, and z = 0.28 for Th (2c) and 0.63 for Bi2 (2c) for $ThBi_2$ [5].

3. Experimental results and analyses

We measured the specific heat C by the thermal relaxation method down to 0.4 K, as shown in **Figure 2**. The specific heat decreases steeply with decreasing temperature. The solid line in Figure 2 is a fitting curve based on an electronic specific heat γT, the phonon contribution βT^3, and the nuclear contribution of Sb and Bi based on the electric quadrupole term A/T^2, namely $C = \gamma T + \beta T^3 + A/T^2$. We obtained the electronic specific heat coefficient γ, the Debye temperature Θ_D, and the coefficient A as 2.6 mJ/(K^2·mol), 151 K, and 0.050 mJ·K/mol for $ThSb_2$ and 3.3 mJ/(K^2·mol), 151 K, and 0.18 mJ·K/mol for $ThBi_2$.

We carried out the dHvA experiment by the field-modulation method with a frequency of 55.8 Hz and a modulation field of 83 Oe. **Figure 3(a)** shows the typical dHvA oscillations for the magnetic field along H ∥ [001] in $ThSb_2$. The corresponding fast Fourier transformation (FFT) spectrum is shown in **Figure 3(b)**. Several dHvA branches named α, α′, β, β′, γ, and the others are observed, with the dHvA frequencies ranging from $F = 1.88 \times 10^6$ to 9.74×10^7 Oe, as shown in Figure 3(b). Here, the dHvA frequency F (= $c\hbar S_F/2\pi e$) is proportional to the maximum or minimum cross-sectional area S_F of the Fermi surface, which is shown as a unit of magnetic field. We rotated the sample against the magnetic field, and obtained the angular dependences of the dHvA frequencies, as shown in **Figure 4(a)**. Solid lines are guides connecting the data. The detected dHvA branches α and α′ are due to cylindrical parts of Fermi surfaces. Branch γ is due to a closed small Fermi surface.

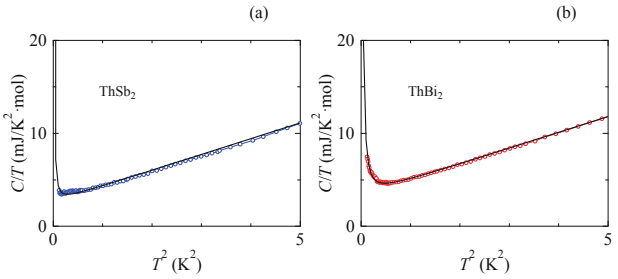

Figure 2. T^2 dependence of the specific heat C in the form of C/T for (a) $ThSb_2$ and (b) $ThBi_2$.

The cyclotron effective masses m^*_c for the dHvA branches were determined from the temperature dependences of the dHvA amplitudes. The cyclotron masses are in the range from 0.11 to 1.02 m_0 (m_0: rest mass of an electron) in $ThSb_2$, summarized in **Table 2**.

To clarify the Fermi surface properties, we have

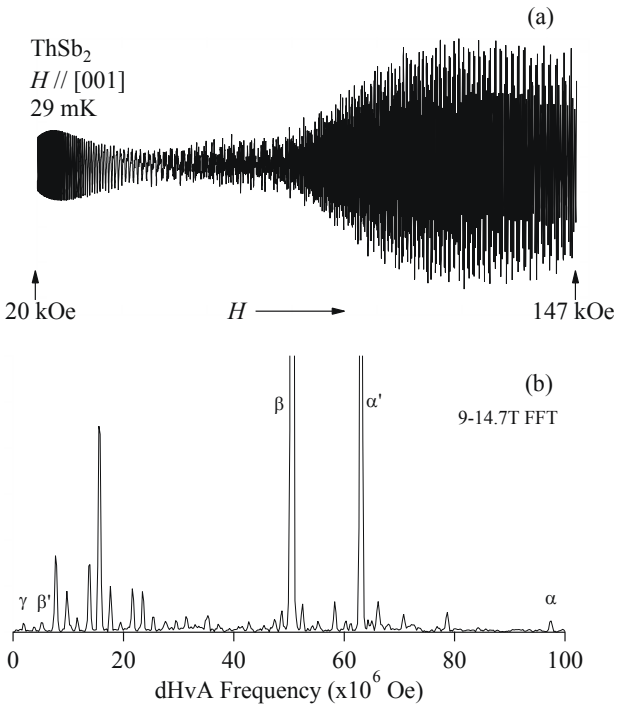

Figure 3. (a) Typical dHvA oscillations for H ∥ [001] and (b) the corresponding FFT spectrum in $ThSb_2$.

Table 1. Lattice parameters and atomic positions at room temperature in $ThSb_2$, where R and wR are the reliability factors, and B is the equivalent isotropic atomic displacement parameter.

Space group	Lattice parameter (Å)	Atom (site)	Position x, y, z	B
$P4/nmm$ (D^7_{4h}) No. 129 (R=6.45, wR=17.41)	a=4.3512 c=9.1853	Th (2c) Sb1(2a) Sb2(2c)	0, 1/2, 0.2741 0, 0, 0 1/2, 0, 0.6297	0.41 0.59 0.54

Table 2. dHvA frequencies F and the cyclotron masses m^*_c for H ∥ [001] in $ThSb_2$, together with the theoretical dHvA frequencies F_b and the band masses m_b. See the text for the details of calculations.

	Experiment		Theory (LDA)		Theory (LDA+5f 0.2Ry)	
	F(×10^7 Oe)	$m^*_c(m_0)$	F_b(×10^7 Oe)	$m_b(m_0)$	F_b(×10^7 Oe)	$m_b(m_0)$
α	9.739	0.78	9.817	0.834	9.587	0.702
α'	6.304	1.02	6.297	0.874	6.154	0.745
β	5.054	0.57	5.254	0.470	5.062	0.441
β'	0.514	0.29	0.361	0.351	0.442	0.280
γ	0.188	0.11	0.217	0.088	0.210	0.078

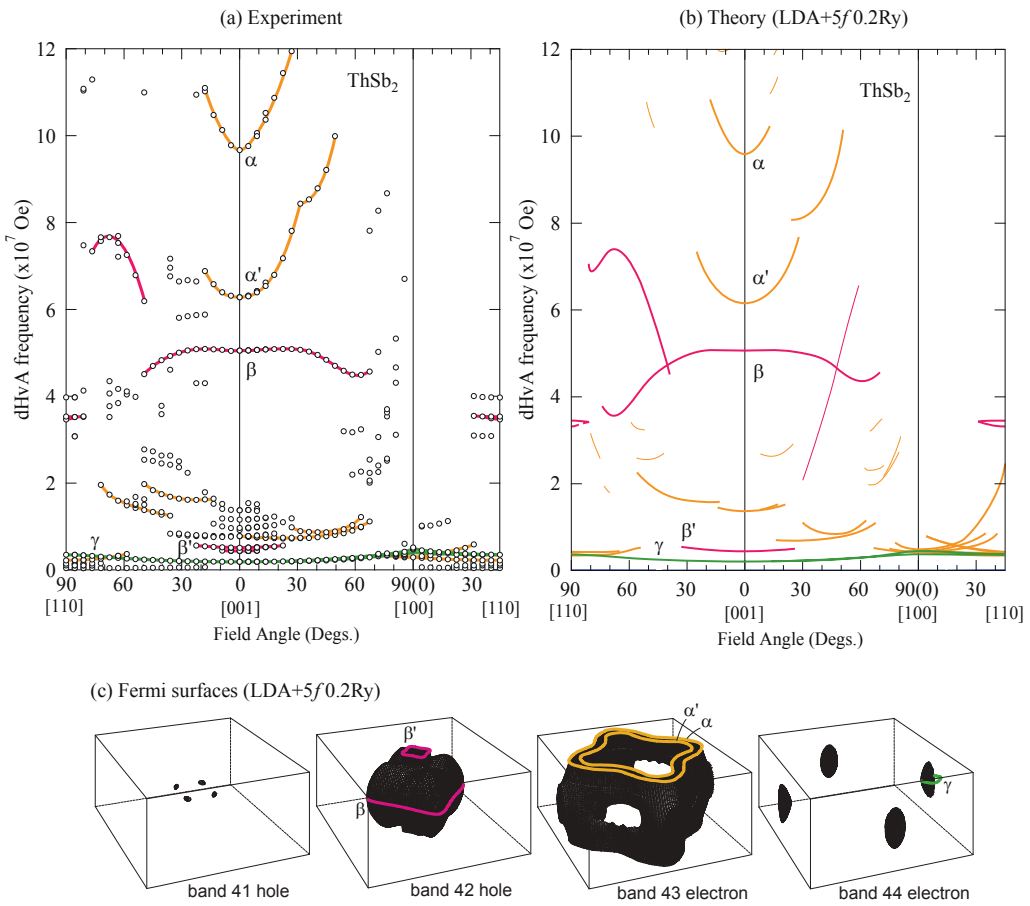

Figure 4. Angular dependences of (a) dHvA frequencies, (b) the theoretical ones (LDA+5*f* 0.2Ry), and (c) the corresponding theoretical Fermi surfaces in $ThSb_2$.

calculated the energy band structure for $ThSb_2$ by using the full-potential linearized augmented plane wave (FLAPW) method with the local density approximation (LDA) for the exchange correlation potential. We have also tried to shift 5*f* level in Th to reproduce the γ value, properly. In the present band calculation, the scalar relativistic effect was taken into account for all the electrons, and then the spin-orbit coupling was included self-consistently for all the valence electrons as in a second variational procedure. $6s^26p^66d^27s^2$ electrons for Th and $4d^{10}5s^25p^3$ electrons for Sb are treated as valence electrons in the calculation. The space group and lattice parameter are adopted from Table 1. **Figures 4(b)** and **(c)** show the theoretical angular dependences of dHvA frequencies F_b, and the corresponding Fermi surfaces, respectively. Here, we have used an upward shifted potential by 0.2 Ry, for the 5*f* electrons in Th. A reason of this correction is described later. The detected dHvA branches are identified as follows:

1) Branches α and α′ are due to outer and inner orbits of the band 43-electron Fermi surface, respectively.
2) Branches β and β′ are due to a belly orbit of a flat closed band 42-hole Fermi surface and a small neck Fermi surface, respectively.
3) Branch γ is due to a small band 44-electron Fermi surface.

Here, we note why we introduced the extra potential for the 5*f* electrons in Th. If we simply calculate the band calculation on the basis of LDA, we obtained the theoretical γ_b value of γ_b = 2.83 mJ/(K^2·mol). This value is larger than the experimental value of γ = 2.6(±0.03) mJ/(K^2·mol). This value of 2.83 mJ/(K^2·mol) is usually much enhanced by the electron-phonon interaction, most likely reaching 3.0 mJ/(K^2·mol) in reality. The theoretical γ value should be smaller than the experimental one. The obtained larger γ value is mainly due to a tail of the partial density of states of Th-5*f* electrons, which are mainly unoccupied above the Fermi energy E_F. We therefore shifted the 5*f* level upward by 0.2 Ry to reduce the effect of 5*f* bands in Th. The corresponding theoretical γ_b value is γ_b = 2.33 mJ/(K^2·mol), which is consistent with the experimental value of γ = 2.6 mJ/(K^2·mol). This treatment has been once introduced to the energy band calculation of $ThIn_3$ [6]. Then, the Fermi surfaces are reproduced properly.

We also show in **Figure 5** the total and partial density of states, which was calculated on the basis of LDA+5*f* 0.2Ry. The Fermi surfaces are mainly composed from Sb-5*p* electrons, together with a small contribution of Th-6*d* and -5*f* electrons.

Similarly, we measured the dHvA oscillations in $ThBi_2$. We show in **Figure 6** the angular dependences of the dHvA frequencies in $ThBi_2$, which are almost the same as those of $ThSb_2$. The dHvA frequencies in $ThBi_2$

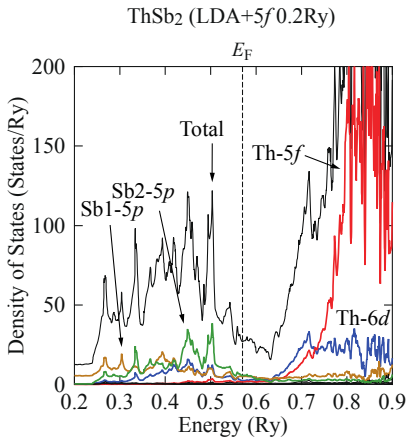

Figure 5. Density of states in $ThSb_2$ based on LDA+5*f* 0.2Ry.

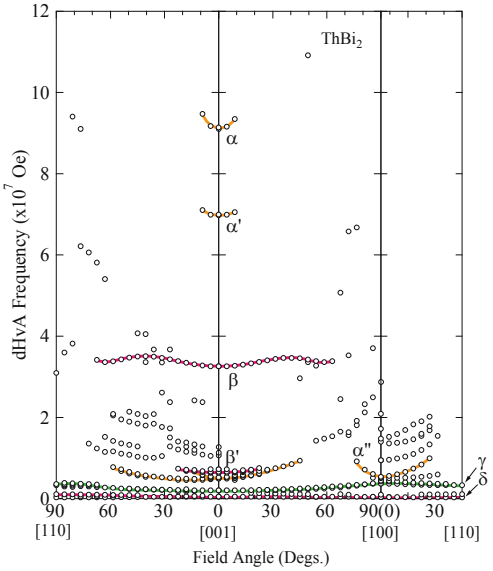

Figure 6. Angular dependences of dHvA frequencies in $ThBi_2$.

are, however, slightly smaller than those in $ThSb_2$. The cyclotron masses in $ThBi_2$ are found to be larger than those of $ThSb_2$, as shown in **Figure 7**. The electronic specific heat coefficient γ in $ThBi_2$ is also larger than the one in $ThSb_2$, $\gamma_{ThBi2}/\gamma_{ThSb2}$ = 1.4, as shown in Figure 2. This is a characteristic feature. We will discuss this point.

Bi-6*p* electrons and Sb-5*p* electrons become main conduction electrons in $ThBi_2$ and $ThSb_2$, respectively. The lattice constants of $ThBi_2$ are larger than those of $ThSb_2$, as mentioned in Sec. 2. This brings about a small band width in $ThBi_2$, compared with the one in $ThSb_2$, although the wave function of 6*p* in Bi is extended more than that of 5*p* in Sb. This is a main reason why the band mass or the cyclotron mass in $ThBi_2$ is larger than the one in $ThSb_2$.

4. Concluding remark

We grew single crystal of $ThSb_2$ and $ThBi_2$ and

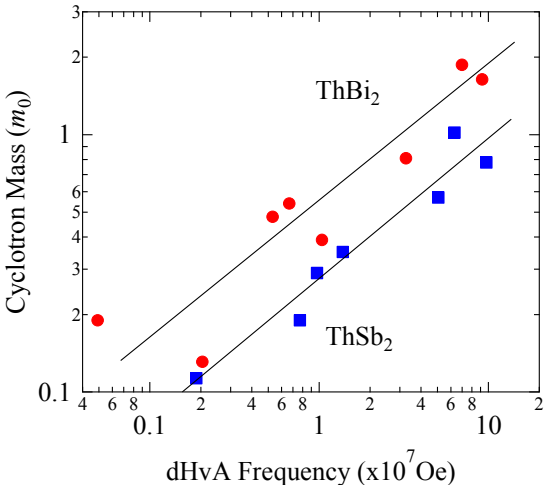

Figure 7. Relation between the cyclotron masses and dHvA frequencies for $ThSb_2$ and $ThBi_2$.

studied the Fermi surface properties. The cyclotron masses are in the range from 0.11 to 1.02 m_0 (m_0: rest mass of an electron) in $ThSb_2$ and from 0.13 to 1.87 m_0 in $ThBi_2$, respectively. The cyclotron masses of $ThBi_2$ are large compared with those of $ThSb_2$. This might be due to a small band width of $ThBi_2$, compared with the one of $ThSb_2$, reflecting large lattice constants of $ThBi_2$, compared with those of $ThSb_2$. In the present band calculation, we introduced an extra potential for the 5*f* electrons in Th to shift the 5*f* level upward in energy. It is important to determine experimentally the correct energy position of the Th-5*f* electrons in the energy dispersion, which is left to the future study.

Acknowledgements

This work was supported by JSPS KAKENHI Grant Numbers JP25247055, JP15K05156, JP15H05884, JP15H05882, JP16H04006, JP16K17733, and JP16H01078 and start-up research costs from the Project to Promote Gender Equality and Support Female Researchers from Tohoku University.

References

[1] Y. Haga, E. Yamamoto, Y. Tokiwa, D. Aoki, Y. Inada, R. Settai, T. Maehira, H. Yamagami, H. Harima and Y. Ōnuki, *J. Nucl. Sci. Technol., Suppl.* 3 (2002), pp. 56-62.

[2] T. D. Matsuda, Y. Haga, E. Yamamoto, S. Ikeda, H. Shishido, R. Settai, H. Harima and Y. Ōnuki, *J. Phys. Soc. Jpn*. 76 (2007), p. 064712(1-7).

[3] Y. Ōnuki and R. Settai, *Low Temp. Phys*. 38 (2012), pp. 119-190.

[4] R. Ferro, *Acta Cryst*. 9 (1956), pp. 817-818.

[5] R. Ferro, *Acta Cryst*. 10 (1957), pp. 476-477.

[6] T. D. Matsuda, Y. Haga, S. Ikeda, H. Shishido, R. Settai, H. Harima and Y. Ōnuki, *J. Phys. Soc. Jpn*. 74 (2005), pp. 3276-3282.